EUROPHYSICS LETTERS 15 February 2000

Europhys. Lett., **49** (4), pp. 431–437 (2000)

The shape of polymer-decorated membranes

M. Breidenich, R. R. Netz and R. Lipowsky

Max-Planck-Institut für Kolloid- und Grenzflächenforschung
Am Mühlenberg, 14476 Golm, Germany

(received 5 August 1999; accepted in final form 2 December 1999)

PACS. 36.20.-r – Macromolecules and polymer molecules.
PACS. 05.40.-a – Fluctuation phenomena, random processes, noise and Brownian motion.
PACS. 82.70.-y – Disperse systems.

Abstract. – Flexible membranes with anchored polymers are studied using both analytical methods and Monte Carlo simulations. The anchored polymers exert an entropically induced pressure on the membrane which is calculated explicitly using a small-gradient expansion. Likewise, we are able to determine both the shape profile of the membrane, which approaches a cone-like shape close to the anchor and a catenoid far away from it, and the profile of the induced mean curvature. We also consider membranes decorated by many polymers and identify two coverage regimes; one of which is governed by polymer/membrane and the other by polymer/polymer interactions.

At the supramolecular scale, biological systems consist of different types of macromolecules and biocolloids [1,2]. These structures experience a variety of weak and competing interactions which lead to many levels of supramolecular organization. Biomimetic systems are model systems which are constructed and studied in order to focus on certain aspects of this self-organization. Two relatively simple examples for such systems are provided by water-soluble polymers and lipid bilayer membranes, both of which exhibit an interesting combination of flexibility and structural stability. New levels of self-organization are found in compound systems which are composed of both membranes and polymers attached to these membranes via anchor segments, for a short review, see [3].

Systems composed of lipid membranes with anchored polymers have been studied by various experimental methods [4–8]. It was found in these experimental studies that anchored polymers can have drastic effects on the shape of the lipid membranes. From a theoretical point of view, it was shown that the anchored polymer exerts an entropic force on the membrane which bends the membrane away from the polymer [9,10]. So far, the membrane shape arising from this entropic interaction has not been determined. In this article, we develop a theoretical approach with which we can calculate analytically this shape to first order in a small gradient expansion. As shown below, the resulting shape is cone-like close to the polymer anchor and a catenoid far away from it.

In addition to these analytical calculations, we performed extensive Monte Carlo (MC) simulations of the compound polymer/membrane system. In order to give some intuitive idea about the behaviour of this system, we summarize the results of the MC simulations in figs. 1,

© EDP Sciences

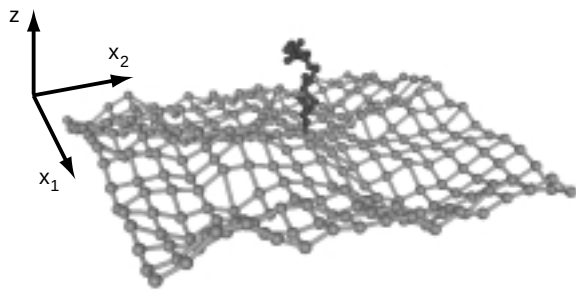

Fig. 1 – Snapshot configuration after 10^4 MC steps. The lateral membrane size is four times larger than the polymer end-to-end distance. The membrane contains $17 \times 17 = 289$ lattice sites and the polymer consists of 33 beads. Bending rigidity $\kappa/T = 1$, harmonic potential parameter $v_2 {R_\mathrm{p}}^4/T = 2$.

2(a) and (b), where we show a typical MC configuration of the compound system, the average MC profile of the membrane and the segment density of the anchored polymer, respectively.

In the main part of this article, we first describe the analytical calculation of the membrane shape induced by the polymer. These analytical results are then compared with the results obtained from the MC simulations. Finally, we also estimate the effective interaction between two anchored polymers arising from the membrane fluctuations.

The compound polymer/membrane system is characterized by: i) the bending rigidity of the membrane, which measures the energy needed to curve a piece of membrane [11]; ii) the end-to-end distance of the polymer R_p, which is related to the mean squared distance between the first and the last monomer in the chain. The chains are treated as ideal or Gaussian, *i.e.*, we ignore any effects from the excluded volume of the polymers. Experimentally, this situation corresponds to a polymer in a solvent close to the θ-temperature, where the excluded-volume effect is balanced by the attractive interaction between polymer segments due to van der Waals forces. For the ideal chain, one has $R_\mathrm{p} = a_\mathrm{p}\sqrt{N}$, where a_p and N are the persistence length and the total number of monomers, respectively.

Now, we will calculate the mean profile of the membrane with an anchored polymer by a perturbation expansion. The membrane is not subject to any additional forces or constraints

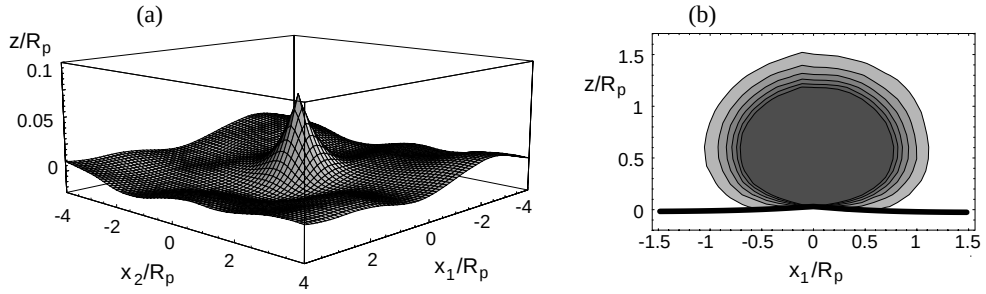

Fig. 2 – (a) Membrane profile averaged over 10^7 MC steps. The lateral membrane size is 8 times the polymer end-to-end distance. Bending rigidity $\kappa/T = 1$, harmonic potential parameter $v_2 {R_\mathrm{p}}^4/T = 2$. The membrane contains $65 \times 65 = 4225$ lattice sites, the polymer has 65 beads. (b) The segment density of the polymer on top of the membrane cut in the x_1-direction. The density is obtained by counting the probability of polymer beads to be localized at position $(x_1/R_\mathrm{p}, z/R_\mathrm{p})$ in the cut-plane. The parameters have the same values as in (a).

arising, *e.g.*, from its boundaries. Thus, it is tensionless [1] and governed by its bending rigidity κ; it is parametrized by its surface height $l(\underline{x})$, where $\underline{x} = (x_1, x_2)$ is the plane of reference. The membrane Hamiltonian is then given by

$$\mathcal{H}_{\rm me}\{l\} \;=\; \int \mathrm{d}^2x\, \frac{1}{2}\left(\kappa\left(\nabla^2 l(\underline{x})\right)^2 + v_2 l(\underline{x})^2\right)\,. \tag{1}$$

In order to organize the calculation, we added a harmonic potential of strength v_2. The physical case corresponds to the limit of vanishing v_2 as explicitly discussed below.

The internal length of the polymer is parametrized by s with $0 \le s \le 1$ where Ns is the number of monomers between the anchor and the polymer segment labeled by s. The polymer partition function is given by

$$\mathcal{Z}_{\rm p}\{l\} \;=\; \int' \mathcal{D}\{\mathbf{r}\}\, \delta[r_1(0)]\, \delta[r_2(0)]\, \delta[r_3(0) - l(\underline{0})]\, \exp\left[-\frac{3}{2R_{\rm p}^2}\int_0^1 \mathrm{d}s\, [\mathrm{d}\mathbf{r}(s)/\mathrm{d}s]^2\right]\,, \tag{2}$$

where the prime at the path integration indicates that $r_3(s) \ge l(r_1(s), r_2(s))$. The partition function of the compound system now has the general path integral form

$$\mathcal{Z} \;=\; \int \mathcal{D}\{l\}\, \exp[-\mathcal{H}_{\rm me}\{l\}/T]\; \mathcal{Z}_{\rm p}\{l\}\,, \tag{3}$$

where T denotes the temperature in energy units. We normalize the polymer partition function $\mathcal{Z}_{\rm p}\{l\}$ by the half-space partition function $\mathcal{Z}_{\rm p}\{l = 0\}$ of a polymer anchored on a flat surface [12]. Expanding the partition function $\mathcal{Z}_{\rm p}$ to first order in l and integrating out the polymer's degrees of freedom, one obtains after some computation the explicit expression

$$\frac{\mathcal{Z}_{\rm p}\{l\}}{\mathcal{Z}_{\rm p}\{0\}} \;\approx\; 1 \;-\; \int_0^1 \mathrm{d}s \int_{-\infty}^{\infty} \mathrm{d}^2x\; P(s, \underline{x})\; l(\underline{x})\,, \tag{4}$$

with the total pressure

$$P(\underline{x}) \;=\; \int_0^1 \mathrm{d}s\; P(s, \underline{x}) = \begin{cases} \dfrac{1}{2\pi x^3}\left(1 + 3\dfrac{x^2}{R_{\rm p}^2}\right)\exp\left[-\dfrac{3}{2}\dfrac{x^2}{R_{\rm p}^2}\right]\,, & \text{for} \quad x > 0\,, \\ -\infty\,, \quad \text{for} \quad x = 0\,, \end{cases} \tag{5}$$

where $x = |\underline{x}|$. The explicit form of the pressure is consistent with the intuitive picture that the polymer pulls the membrane at the anchor point and pushes the membrane away from it.

It follows from the explicit path integral expression for the first-order term that the expansion used here is, in fact, an expansion in powers of the derivatives $\partial l/\partial x_1$ and $\partial l/\partial x_2$ which implies that this term is invariant under the transformation $l(\underline{x}) \to l(\underline{x}) + \Delta l$ of the shape profile. As a consequence, one must have $\int \mathrm{d}^2x\, P(s, \underline{x}) = 0$ for any polymer segment s as can be verified for the explicit form given by

$$P(s, \underline{x}) = \frac{2}{{R_{\rm p}}^3}\left(\frac{3}{2\pi}\right)^{3/2}\left(\frac{1-s}{s}\right)^{1/2}\left(\frac{3}{2}\frac{x^2}{{R_{\rm p}}^2}\frac{1}{s^3} - \frac{1}{s^2}\right)\exp\left[-\frac{3}{2}\frac{x^2}{{R_{\rm p}}^2 s}\right]\,. \tag{6}$$

Note that, for fixed s, $P(s, \underline{x})$ is negative and positive for small and for large x, respectively.

---

[1] A lateral tension Σ introduces the additional crossover length scale $\xi_* = (\kappa/\Sigma)^{1/2}$. The shape profile derived here for the tensionless case also applies for the tense membrane on length scales $x \ll \xi_*$.

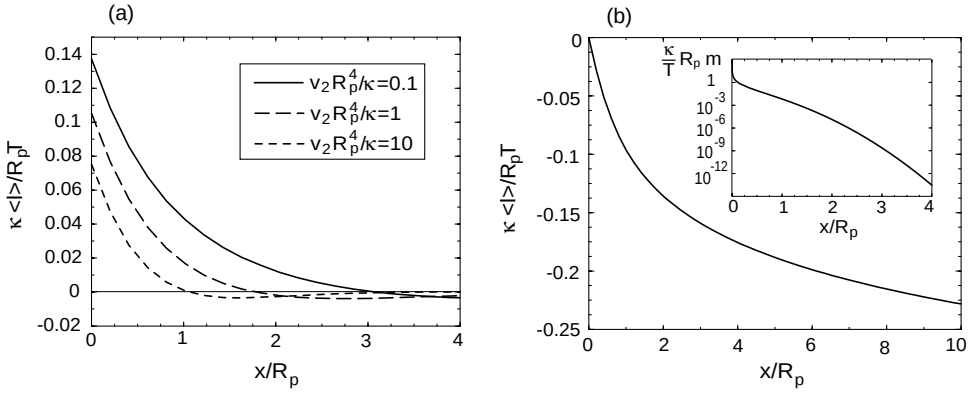

Fig. 3 – The profile of the membrane as obtained by the perturbative calculation: (a) for different nonvanishing values of $v_2{R_\mathrm{p}}^4/\kappa$, (b) for vanishing v_2. The inset displays the corresponding curvature in a linear-logarithmic plot.

Using the polar symmetry of our problem, the average height of the membrane is given by

$$\begin{aligned}\langle l(\underline{x})\rangle \;&=\; \frac{1}{2}\sqrt{\frac{\pi}{6}}\frac{T}{\kappa}R_\mathrm{p}\int_0^\infty \frac{\mathrm{d}q}{2\pi}\frac{q^3}{(q^4+v_2/\kappa)}\times \\ &\quad\times\exp\left[-\frac{R_\mathrm{p}^2}{12}q^2\right]\left[I_0\left(\frac{R_\mathrm{p}^2}{12}q^2\right)+I_1\left(\frac{R_\mathrm{p}^2}{12}q^2\right)\right]\,J_0(qx)\,,\end{aligned} \tag{7}$$

where J_0, I_0, I_1 denote Bessel functions of integer order [13]. The shape profile $\langle l(\underline{x})\rangle$ as given by (7) is shown in fig. 3(a) for different nonvanishing values of $v_2{R_\mathrm{p}}^4/\kappa$. It is obvious, that the height of the membrane must increase with decreasing v_2. As long as the potential is present, the membrane will be localized at $\langle l(\underline{x})\rangle = 0$ for large x. This limit is approached by exponentially damped oscillations. The height of the anchor is given by $\langle l(\underline{x}=\underline{0})\rangle$. In order to consider the limit of small confining potential, *i.e.*, of small v_2, it is useful to shift the coordinate system in such a way that the anchor is located at the origin. In the latter coordinate system, the height profile is given by $\langle l(\underline{x})\rangle - \langle l(\underline{0})\rangle$ which stays finite in the limit of zero v_2. In the latter limit, one finds

$$\begin{aligned}\langle l(\underline{x})\rangle-\langle l(\underline{0})\rangle \;&=\; -\frac{R_\mathrm{p}}{8\pi}\frac{T}{\kappa}\left\{\frac{x}{R_\mathrm{p}}\exp\left[-\frac{3}{2}\frac{x^2}{{R_\mathrm{p}}^2}\right]+\sqrt{\frac{\pi}{6}}\left[\left(1+3\frac{x^2}{{R_\mathrm{p}}^2}\right)\mathrm{erf}\left(\sqrt{\frac{3}{2}}\frac{x}{R_\mathrm{p}}\right)-3\frac{x^2}{{R_\mathrm{p}}^2}\right]+\right. \\ &\quad\left.+\,2\left(\frac{x}{R_\mathrm{p}}\right){}_2F_2\left(\left\{\frac{1}{2},\frac{1}{2}\right\},\left\{\frac{3}{2},\frac{3}{2}\right\},-\frac{3}{2}\frac{x^2}{{R_\mathrm{p}}^2}\right)\right\}\,,\end{aligned} \tag{8}$$

where ${}_2F_2$ is a generalized hypergeometric function [13]. The profile as given by (8) attains the cone-like shape described by

$$\langle l(\underline{x})\rangle - \langle l(\underline{0})\rangle \approx -(T/2\pi\kappa)x\,, \tag{9}$$

for small x, and the catenoid-like shape given by

$$\langle l(\underline{x})\rangle - \langle l(\underline{0})\rangle \approx -(T/\kappa)(R_\mathrm{p}/4\sqrt{6\pi})\ln(x/R_\mathrm{p})\,, \tag{10}$$

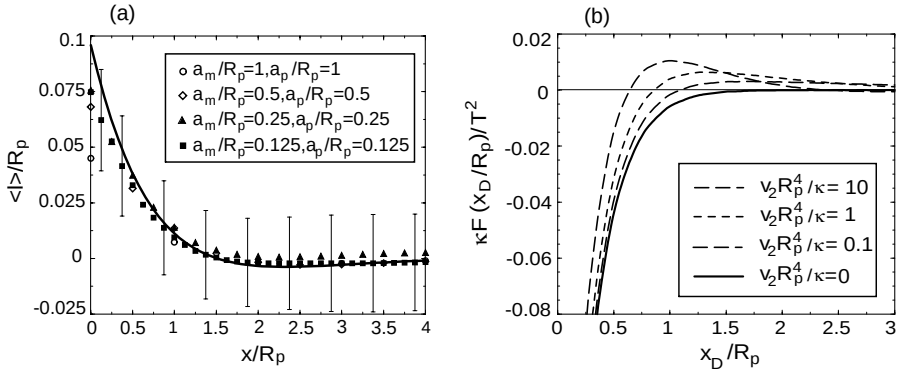

Fig. 4 – (a) Membrane profile: Comparison of analytical calculation (solid line) and Monte Carlo data for different polymer and membrane discretizations $a_\mathrm{p}/R_\mathrm{p}$ and $a_\mathrm{m}/R_\mathrm{p}$, respectively, and $\kappa/T = 1$, $v_2{R_\mathrm{p}}^4/T = 2$. The shape profiles are averaged over 10^7 MC steps. (b) The pairwise, membrane-induced interaction energy between polymers for different values of $v_2{R_\mathrm{p}}^4/\kappa$.

for large x. The profile for $v_2 = 0$ and intermediate x-values is displayed in fig. 3(b).

The mean curvature $m(\underline{x}) = -1/2\langle\nabla^2 l(\underline{x})\rangle$, which we define to be positive if the membrane bends away from the polymer, is shown in the inset of fig. 3(b). The curvature has the asymptotic behavior

$$m(\underline{x}) \approx T/4\pi\kappa x\,, \tag{11}$$

for small x, and

$$m(\underline{x}) \approx (T/12\pi\kappa)({R_\mathrm{p}}^2/x^3)\exp[-3x^2/2{R_\mathrm{p}}^2]\,, \tag{12}$$

for large x. Due to the strong decay of $m(\underline{x})$ for large x, the integral of $m(\underline{x})$ over the infinite plane of reference stays finite and leads to $\int \mathrm{d}^2x\, m(\underline{x}) = \sqrt{\pi/6}(T/4\kappa)R_\mathrm{p}$ for a single anchored polymer as considered so far.

Now, let us consider a membrane of area A which is covered by N_p anchored polymers in the dilute regime. Up to first order in the surface height l, we may simply superimpose the separate shape deformations arising from these polymers ([2]). Thus, for the coverage $\Gamma_\mathrm{p} = N_\mathrm{p}/A$ one obtains the mean (spontaneous) curvature $M_\mathrm{sp} = \sqrt{\pi/6}(T/4\kappa)\Gamma_\mathrm{p}R_\mathrm{p}$.

We will now compare the analytically calculated membrane shape profile with profiles obtained by Monte Carlo simulations, as shown in fig. 4(a). The Monte Carlo simulation was performed using the Metropolis algorithm. The membrane can move continuously in the vertical direction above a two-dimensional lattice with lattice parameter a_m. For the anchored polymer we used the bead-spring model with harmonic spring potential and pointlike beads. The average bond length is given by the persistence length a_p. Periodic boundary conditions have been applied in the lateral directions, which implies that our system consists of a periodic array of anchored polymers. The distance between these polymers which is equal to the lateral membrane size was chosen to be eight times larger than the end-to-end distance of the polymer, which corresponds to a dilute coverage regime (mushroom regime).

As can be seen in fig. 4(a) the simulation data depend on both the polymer discretization a_p and the membrane discretization a_m. The approach to the continuum limit is slow, and

([2]) A similar superposition of membrane deformations has been considered in the so-called hat model in [14].

one has to decrease both length scales simultaneously in order to further reduce the difference between the simulation data and the analytical result.

In the main part of this paper, we have focussed on the membrane degrees of freedom and determined the effective pressure $P(\underline{x})$ arising from the polymer configurations. It is also of interest to assume a different viewpoint in which one focusses on the polymers and determines the effective interactions between these polymers arising from the membrane fluctuations. A similar approach has been used for the effective interactions between membrane inclusions [15, 16]. We start from the partition function (3) where $\mathcal{Z}_{\rm p}$ is now given by

$$\mathcal{Z}_{\rm p}\{l\} \;=\; \exp\left[-\sum_{i=1}^{N_{\rm p}}\int {\rm d}^2x\, P(\underline{x}-\underline{x}_i)\, l(\underline{x})\right]\,, \tag{13}$$

and perform the path integral over all l-configurations. Using the methods of [16], we find the effective pair interaction

$$\begin{aligned}\mathcal{F}(x_D) \;=\; & -\frac{R_{\rm p}^2}{48}\frac{T^2}{\kappa}\int_0^\infty {\rm d}q\,\frac{q^5}{(q^4+v_2/\kappa)}\,\times \\ & \times\exp\left[-\frac{R_{\rm p}^2}{6}q^2\right]\left[I_0\left(\frac{R_{\rm p}^2}{12}q^2\right)+I_1\left(\frac{R_{\rm p}^2}{12}q^2\right)\right]^2 J_0(qx_D)\,,\end{aligned} \tag{14}$$

between two polymers at separation x_D. In fig. 4(b) the interaction energy is shown for different values of $v_2{R_{\rm p}}^4/\kappa$. For small distances, it is always attractive. As long as v_2 does not vanish, one also finds regions with repulsive interaction due to damped oscillations in $\mathcal{F}$. For vanishing v_2, the interaction energy is monotonic and attractive for all values of x_D. The interaction vanishes for stiff membranes because of $\mathcal{F}(x_D)/T \sim T/\kappa$, as we expect for this fluctuation-induced phenomenon. However, the attractive tail in $\mathcal{F}(x_D)$ occurs for distances of the order of $R_{\rm p}$ and smaller, where the polymers intersect. Therefore, if we include excluded-volume effects between the polymers, the attraction interaction will be strongly suppressed.

In order to compare our previous results on the spontaneous curvature of membranes with experiments we will now focus on vesicles with attached polymers, since it is possible to deduce changes in the spontaneous curvature of vesicles by examining their shape transformations [17]. We will consider three contributions to the spontaneous curvature of vesicles: i) We already calculated the spontaneous curvature $M_{\rm sp}^{\rm (pm)} = \sqrt{\pi/6}(T/4\kappa)\Gamma_{\rm p}R_{\rm p}$ from mushroom/membrane interactions. This contribution is linear in the coverage density $\Gamma_{\rm p}$. ii) A second contribution, which is also linear in $\Gamma_{\rm p}$, arises from the size and geometry of the anchor molecules inserted into the membrane. If there is no exchange of molecules between both monolayers (flip-flops) one has $M_{\rm sp}^{\rm (an)} = \Gamma_{\rm p}A_{\rm an}/2l_{\rm me}$, where $A_{\rm an}$ is the lateral anchor area (≈ 0.7 nm^2) and $l_{\rm me}$ is the thickness of the bilayer (≈ 4 nm). iii) A third contribution becomes important, if the mushrooms start to squeeze each other because of excluded-volume effects. In a low-density approximation the repulsive polymer/polymer interaction is characterized by the second virial coefficient b_2, which in this case is given by $b_2 = 4\pi{R_{\rm p}}^2$. Minimizing the sum of both the repulsive interaction free energy and the free energy of bending of the membrane leads to the spontaneous curvature $M_{\rm sp}^{\rm (pp)} = b_2{\Gamma_{\rm p}}^2R_{\rm p}T/4\kappa$. This contribution is quadratic in the coverage density $\Gamma_{\rm p}$. Equating the spontaneous curvature contributions from polymer/membrane and polymer/polymer interactions gives an estimated crossover coverage $\Gamma_{\rm p}^* \simeq 1/4\sqrt{6\pi}{R_{\rm p}}^2$, which is proportional to but smaller than the overlap concentration $\Gamma_{\rm p}^{\rm (ov)} = 1/\pi R_{\rm p}^2$. In this way, one can identify two different mushroom regimes 1 and 2. Regime 1 with $\Gamma_{\rm p} < \Gamma_{\rm p}^*$ is dominated by

the entropically induced polymer/membrane interaction. Regime 2 with $\Gamma_{\rm p} > \Gamma_{\rm p}^*$ is governed by the polymer/polymer interaction arising from the excluded volume.

For a typical polymer end-to-end distance $R_{\rm p} = 10^{-2}\mu$m and a giant vesicle radius $R_{\rm ve} = 10\ \mu$m, a coverage density $\Gamma_{\rm p}$ of about ten percent of the overlap coverage and a bending rigidity of $\kappa/T = 10$ all three contributions discussed above are of comparable size. We find $M_{\rm sp}^{\rm (pm)} \approx 0.06\ \mu{\rm m}^{-1}$, $M_{\rm sp}^{\rm (an)} \approx 0.03\ \mu{\rm m}^{-1}$ and $M_{\rm sp}^{\rm (pp)} \approx 0.03\ \mu{\rm m}^{-1}$. For the total reduced curvature $(M_{\rm sp}^{\rm (pm)} + M_{\rm sp}^{\rm (an)} + M_{\rm sp}^{\rm (pp)})R_{\rm ve}$, which determines the equilibrium shape of the vesicle, we find a value of about 1.2, which according to the area-difference-elasticity model presented in [17] leads to a measurable change in the shape of vesicles.

In summary, we have introduced a theoretical approach with which one can explicitly calculate the membrane shape arising from the interaction with anchored polymers. This approach has been applied to the case of linear polymers which are anchored to the membrane at one end. We have derived explicit expressions for the effective pressure which such a polymer exerts on the membrane, see (6), for the resulting shape profile which interpolates between a cone and a catenoid, see (8), (9), (10), and for the mean curvature arising from the polymer/membrane interactions, see (11), (12). The same approach can be applied to other cases such as polymers which either translocate through the membrane, are anchored at both ends, or are adsorbed onto the membrane [18]. Furthermore, one may use the same methods in order to study membranes under lateral tension.

REFERENCES

[1] Hoppe W., Lohmann W., Markl H. and Ziegler H., *Biophysics* (Springer, Berlin) 1983.
[2] Alberts B. *et al.*, *Molecular Biology of the Cell* (Garland Publishing, New York) 1989.
[3] Lipowsky R., *Colloids Surf. A: Physicochem. Eng. Aspects*, **128** (1997) 255.
[4] Decher G., Kuchinka E., Ringsdorf H., Venzmer J., Bitter-Suermann D. and Weisgerber C., *Angew. Makromol. Chem.*, **166/167** (1989) 71.
[5] Simon J., Kühner M., Ringsdorf H. and Sackmann E., *Chem. Phys. Lipids*, **76** (1995) 241.
[6] Frette V., Tsafrir I., Guedeau-Boudeville M.-A., Jullien L., Kandel D. and Stavans J., *Phys. Rev. Lett.*, **83** (1999) 2465.
[7] Jakobs B., Sottmann T., Strey R., Allgaier J., Willner L. and Richter D., *Langmuir*, **15** (1999) 6707.
[8] Döbereiner H.-G., Lehmann A., Goedel W., Selchow O. and Lipowsky R., *Mat. Res. Soc. Symp. Proc.*, **489** (1998) 101.
[9] Lipowsky R., *Europhys. Lett.*, **30** (1995) 197.
[10] Hiergeist C. and Lipowsky R., *J. Phys. II*, **6** (1996) 1465.
[11] Helfrich W., *Z. Naturforsch. C*, **28** (1973) 693.
[12] Eisenriegler E., *Polymers near Surfaces* (World Scientific, Singapore) 1993.
[13] Abramowitz M. and Stegun I., *Handbook of Mathematical Functions* (Dover Publications, New York) 1972; Gradshteyn I. S. and Ryzhik I. M., *Table of Integrals, Series and Products* (Academic Press, New York) 1980.
[14] Helfrich W., *Liq. Cryst.*, **5** (1989) 1647.
[15] Goulian M., Bruinsma R. and Pincus P., *Europhys. Lett.*, **22** (1993) 145.
[16] Netz R. R., *J. Phys. I*, **7** (1997) 833.
[17] Miao L., Seifert U., Wortis M. and Döbereiner H.-G., *Phys. Rev. E*, **49** (1994) 5389.
[18] Breidenich M., Netz R. R. and Lipowsky R., to be published.